Formation dynamics of $CH_3NH_3PbI_3$ perovskite following two-step layer deposition

*Jay B. Patel, Rebecca L. Milot, Adam D. Wright, Laura M. Herz, and Michael B. Johnston**

Department of Physics, University of Oxford, Clarendon Laboratory, Parks Road, Oxford

OX1 3PU, United Kingdom

Supporting Information

Contents:

1. Sample Preparation

$MAPbI_3$ perovskite thin films

A two-step thermal evaporation technique, which was modified to slow the reaction of PbI_2 and MAI, was used to grow bilayer films of PbI_2 and MAI[1,2] on z-cut quartz, glass and KBr substrates under high vacuum. The tooling factor for the quartz crystal microbalance (QCM) was determined by depositing the PbI_2 and MAI separately and then measuring the thickness using a DEKTAK 150 profiler. The QCM was also used to ensure that the final film had a 1:1 molar ratio by correlating the density of the compounds with the thicknesses measured by an uncalibrated QCM. MAI was synthesized using previously reported methods,[3] and lead(II) iodide, ultra-dry, 99.999% (metals basis) was purchased from Alfa Aesar.

300 mg of MAI and PbI_2 were placed in separate crucibles, and the quartz, glass and KBr substrates were mounted on a rotating substrate holder to ensure that a uniform film was deposited. The chamber was pumped down to a base pressure of 10^{-6} mbar. The substrate temperature was kept at 21°C whilst the deposition of PbI_2 took place at a rate of 0.5 Å/s. After the desired thickness was deposited (200nm), the substrate temperature was lowered to 0°C and kept at constant temperature for 30 minutes. To slow the reaction of PbI_2 and MAI, the substrate temperature was maintained at 0°C while the MAI was deposited at a rate of 1.3 Å/s. The thickness of the layers deposited was 200 nm each, as measured by quartz crystal microbalance during the deposition. Once the deposition was completed the films were kept under high vacuum and at 0°C for 3 hours before being removed from the vacuum chamber. The films were transferred to the spin coater within a nitrogen-filled glovebox (<1 ppm H_2O and O_2). A layer of PMMA (10mg/ml) was then spin coated onto the films at 2000 rpm for 45 seconds to provide a thin protective layer to prevent the films from being directly in contact with the atmosphere. Thereafter the substrates were either mounted in a vacuum cell (for the PL measurements) or taken in an airtight container to the FTIR spectrometer, where they were immediately placed under vacuum in the sample compartment. For XRD measurements, the films were placed in the sample holder, sealed with Kapton® polyimide sheets within the glovebox and then transported to the diffractometer in an airtight container.

Dihydrate thin films:

The dihydrate films were made using dual source evaporation on z-cut quartz and KBr.[4–7] MAI was synthesized using previously reported methods[3]. Lead(II) iodide, ultra-dry, 99.999% (metals basis) was purchased from Alfa Aesar. 300 mg of MAI and PbI_2 were placed in the separate crucibles and the various substrates were mounted on a rotating substrate holder, to ensure a uniform film was deposited. The temperature of the substrates were kept at 21 °C throughout the deposition. The chamber was allowed to reach a high vacuum (10^{-6}mbar), after which the PbI_2 was heated to 250 °C; once the rate was stabilized (0.4 $Ås^{-1}$) the MAI was heated to 100 °C. Once the deposition rate for MAI had stabilized (1.2 $Ås^{-1}$) the substrates were exposed to the vapor for a set amount of time depending on the desired thickness. The rates of both the MAI and PbI_2 depositions were monitored using a quartz crystal microbalance, to ensure a 3:1 molar ratio was achieved in the final composition of the film. The final co-deposition rate was 1.2 $Ås^{-1}$ and the thickness of the films were 250 nm (DEKTAK 150 profiler). The films were then kept in ambient conditions; within 5 minutes the dark perovskite film turned into a grey, opaque film.

Monohydrate Crystals

Monohydrate crystals were made using a previously reported method.[8] Aqueous HI (57 wt% in H_2O, Sigma Aldrich) was added dropwise to a 12ml solution of CH_3NH_2 (40 wt% in H_2O, Sigma Aldrich), until neutralized (pH 7). The mixture was then heated to 100°C and stirred vigorously. A solution of 3.86 g of $Pb(NO_3)_2$ in 18mL of H_2O was then added dropwise to the hot MAI solution. Thereafter the solution was allowed to cool slowly to room temperature over 4 hours, and then the pale yellow crystals were stored in the mother liquor in the refrigerator at 5°C until taken out for a measurements, whereupon they were filtered and dried under vacuum.

2. Details of Measurement Techniques

FTIR measurements

Both the visible and mid-infrared spectra were measured using a Bruker Vertex 80v Fourier-transform infrared (FTIR) spectrometer fitted with a reflection/transmission accessory. Visible measurements were taken using a tungsten halogen lamp source and a silicon diode detector, and mid-infrared measurements were taken using a globar source and a nitrogen-cooled photovoltaic HgCdTe detector. Spectra for the monohydrate crystals were measured in air using an attenuated total reflection accessory.

Time Correlated Single Photon Counting (TCSPC)

The sample was mounted in a vacuum cell ($p < 10^{-5}$ mbar) and photoexcited by a 398 nm picosecond pulsed diode laser (PicoHarp, LDH-D-C-405M) with a repetition rate of 5 MHz and a fluence of 507 nJ/cm^2. The resultant photoluminescence (PL) was collected and focused into a grating monochromator (Princeton Instruments, SP-2558), which directed the PL onto a photon counting detector (PDM series from MPD). The timing was controlled by a PicoHarp 300 TCSPC event timer. PL time decay traces were measured at a wavelength of 780 nm.

X-Ray Diffraction Measurements

2θ measurements were performed using an X-ray diffractometer (Panalytical X'Pert Pro). The scan speed was 0.02 °/s for 30 minutes (Cu-Kα radiation operating at 40 kV and 40 mA). The diffraction patterns were corrected against tilt using quartz as a reference peak (2θ=16.43°) and were fitted using the pseudo-Voigt profile fit function on X'pert Highscore software.

The bilayer samples were kept in a polyimide seal which slowly let in ambient air, and left in the same position for 30 hours to ensure that the same area of the film was characterized.

3. Additional Mid IR Spectra

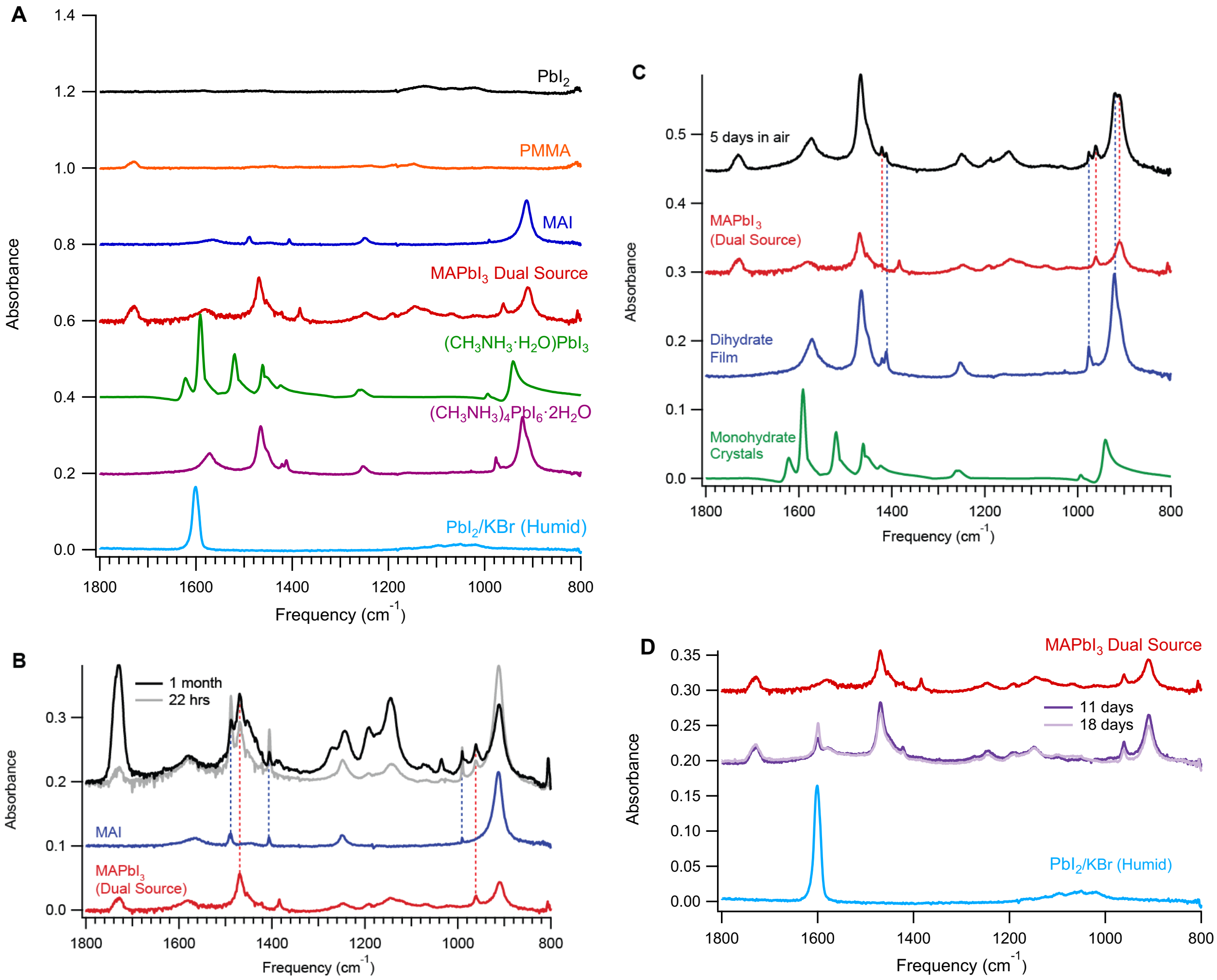

Figure S1. A) The IR spectra for the each of the precursor materials. Details on how they were prepared can be found in Table S1. B) IR spectra of bilayer films kept in vacuum for 22 hours compared with those for a bilayer film kept in a glovebox (<1 ppm O_2, <1 ppm H_2O) for 1 month. Minimal changes are observed, indicating that without a helper molecule such as H_2O, the final $MAPbI_3$ will not form. The increase in intesity at 1732 cm^{-1} and between 1100 cm^{-1} and 1300 cm^{-1} for the 1-month sample is due to a thicker protective layer of PMMA. C) IR spectra used to assign vibrational modes associated with the dihydrate $(CH_3NH_3)_4PbI_6{\cdot}2H_2O$ D) IR spectra to show the initiation of degradation. It is clear from both the appearance of the PbI_2 peak (1600 cm^{-1}) and the diminishing intensity on the $MAPbI_3$ peaks that the films on a KBr substrate are starting to degrade in comparison to a film grown via the dual source method.

4. Additional XRD Measurements

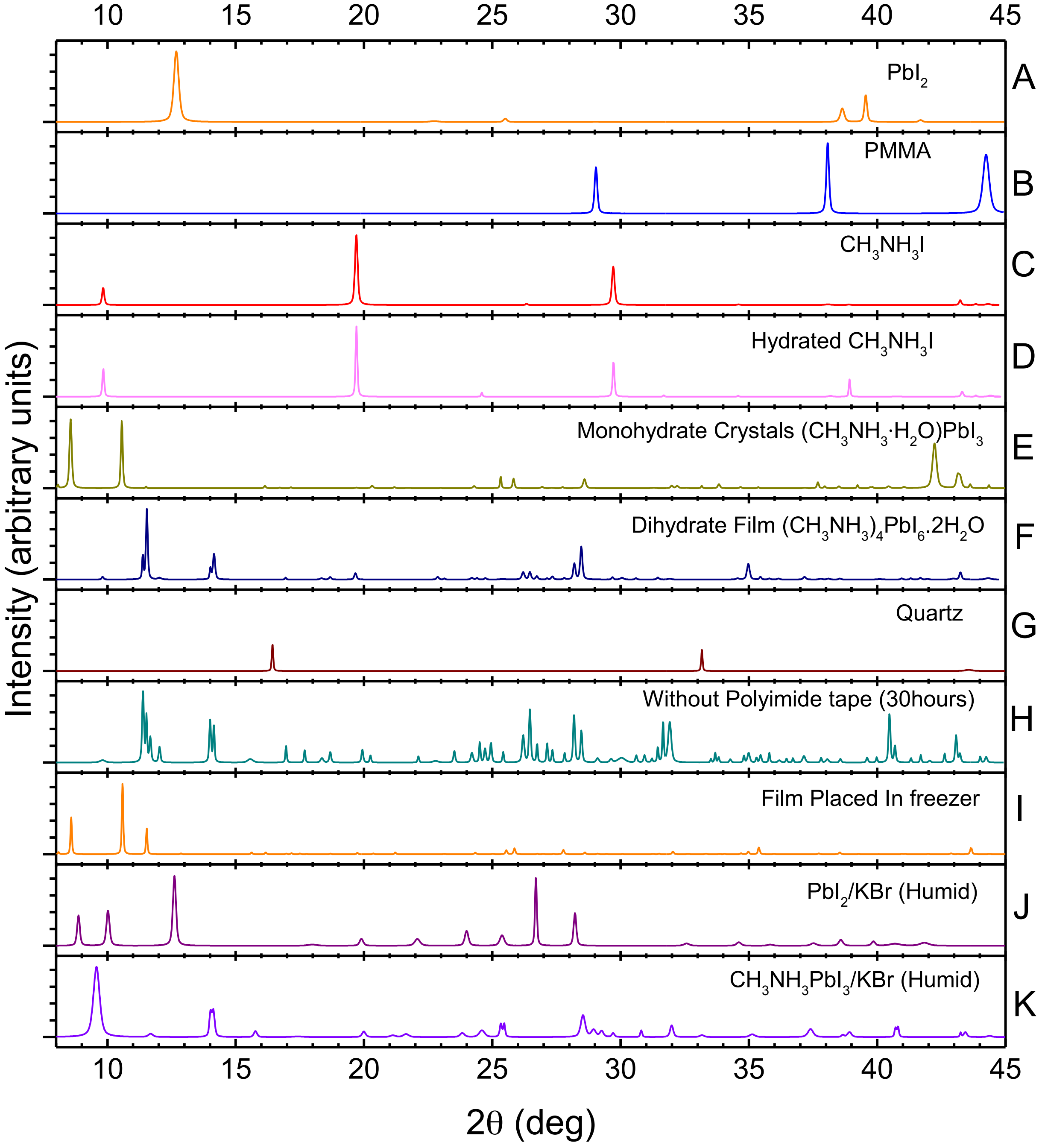

Figure S2. X-Ray diffraction patterns for precursors and derivative compounds associated with intermediates or degradation products of $MAPbI_3$. Details about each sample are provided in Table S1.

Diffraction Pattern	Description
A PbI_2	A thermally evaporated 200nm thin film of PbI_2 with a strong reflection for the (001) plane at $2\theta=12.6°$
B PMMA	A spin coated thin film of Poly(methyl methacrylate)
C MAI	A thermally evaporated 200nm thin film of MAI
D Hydrated MAI	A thermally evaporated 200nm thin film of MAI after exposure to ambient air for 24 hours. Note the formation of peaks at $2\theta=24.8°$ and 39°.
E Monohydrate crystals $(CH_3NH_3{\cdot}H_2O)PbI_3$	Monohydrate crystals $(CH_3NH_3{\cdot}H_2O)PbI_3$ grown from solution as described above. Characteristic peaks are visible at $2\theta= 8.6°$ and 10.6°. There is also a weak peak at $2\theta=11.6°$ corresponding to a dihydrate reflection indicating that the hydrates are in equilibrium with each other and the $MAPbI_3$
F Dihydrate $(CH_3NH_3)_4PbI_6{\cdot}2H_2O$	A thermally evaporated 350nm thin film of the dihydrate $(CH_3NH_3)_4PbI_6{\cdot}2H_2O$ with its characteristic peaks at $2\theta=11.4°$,11.5° and 11.6°
G Quartz	Z-cut quartz used as a substrate for all thin films for XRD measurements. The diffraction patterns were referenced against the standard $2\theta=16.433°$
H Without the polyimide tape	After 30 hours, a diffraction pattern of the characterized film in Figure 2 in the main text is taken without the polyimide tape, to show the clear formation of crystalline dihydrate along with crystalline $MAPbI_3$.
I Film placed in freezer	A thermally evaporated bilayer thin film of MAI/PbI_2 kept at -5°C in ambient air. There is clear formation of both the monohydrate and the dihydrate, and there are no perovskite peaks in the diffraction pattern. Furthermore there are no PbI_2 or MAI peaks, indicating ion diffusion occurs at relatively low temperatures with the aid of moisture. It is also clear that the hydrates form strongly crystalline domains at relatively low temperatures.
J PbI_2/KBr (humid)	A thermally evaporated 200nm thin film of PbI_2 on a KBr window left in a humid environment. Peaks are formed at $2\theta= 8.9°$ and 10.0° which are somewhat similar to that of the monohydrate
K $CH_3NH_3PbI_3$/KBr (humid)	The converted bilayer films used in the main study were left outside for two weeks in a humid environment. Peaks form at $2\theta= 9.6°$ and 11.7°

Table S1: The descriptions of the various diffraction patterns in Figure S2.

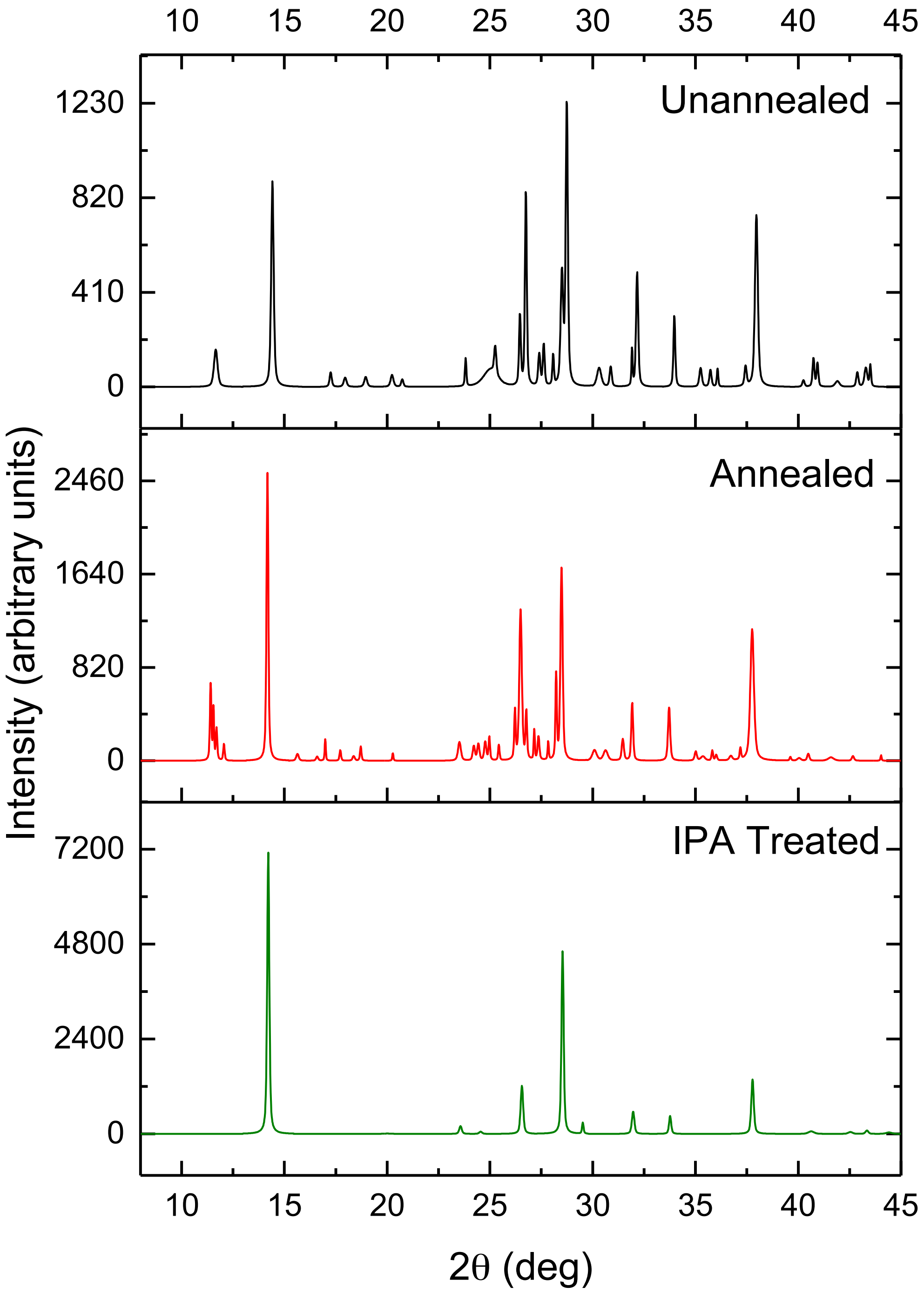

Figure S3: XRD patterns for a $MAPbI_3$ film fabricated via dual source evaporation[7] on fluorine-doped tin oxide (FTO). A dihydrate $(CH_3NH_3)_4PbI_6{\cdot}2H_2O$ is formed after the bilayer film is exposed to ambient air immediately after the fabrication on the film. After annealing in ambient air, the dihydrate peaks remain. Spin coating IPA on the films clearly shows the removal of the dihydrate and a more crystalline film.

5. PL Transients

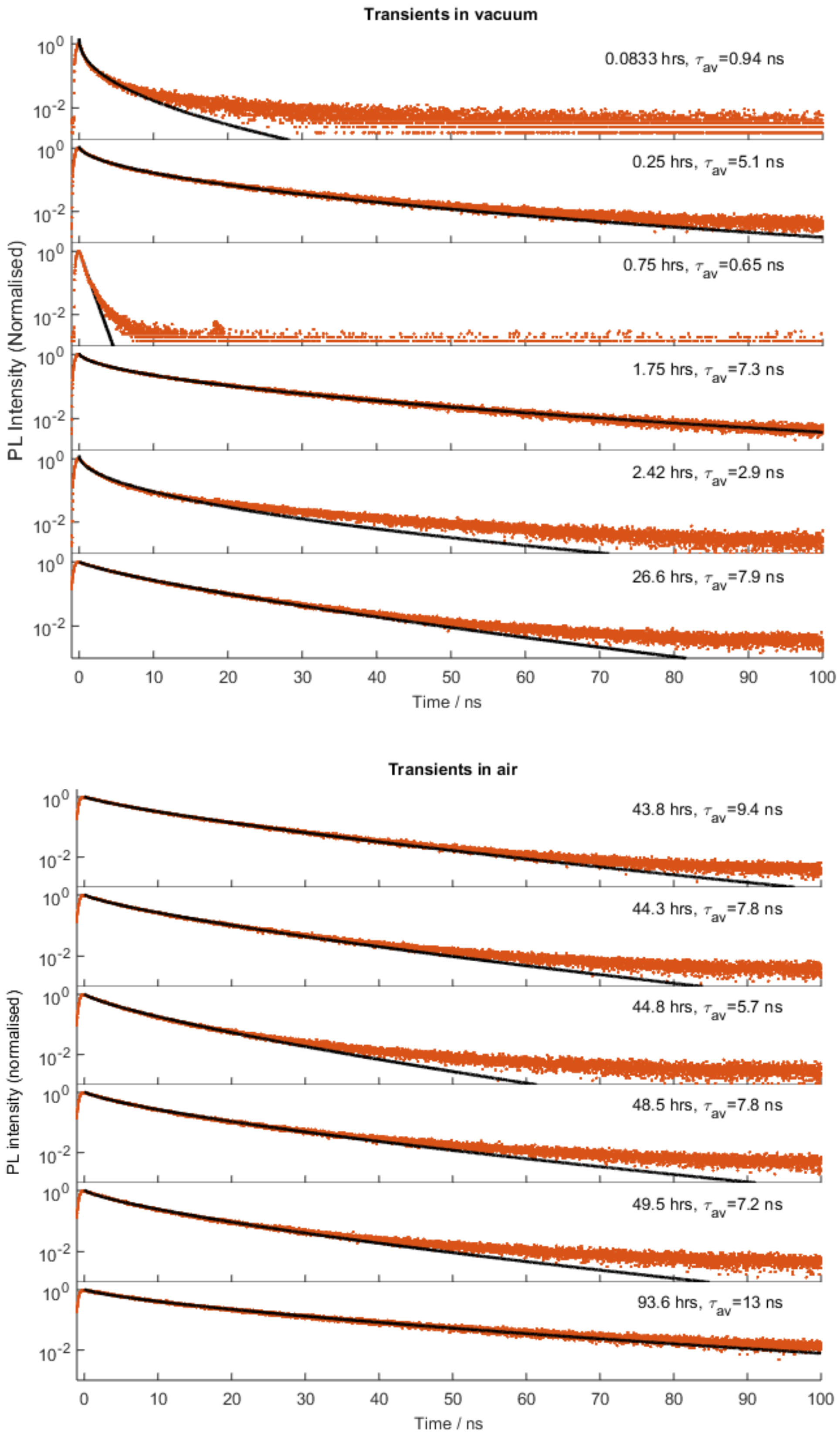

Figure S4. PL transients measured in vacuum and after exposure to ambient air.

The transients were fitted by a stretched exponential function of the form $I(t) = I_0 e^{-(t/\tau_c)^{\beta}}$, where $I(t)$ is the time dependent PL intensity, I_0 is the initial PL intensity, τ_c is the characteristic lifetime of the decay and β is the distribution coefficient. Such stretched exponential functions have previously been used to describe relaxations in terms of a superposition of exponential decays.[9,10] The average lifetime of the fitted stretched exponential functions was calculated using the relationship

$$\tau_{av} = \frac{\tau_c}{\beta} \Gamma \left(\frac{1}{\beta} \right)$$

where Γ is the gamma function. [10]

6. References.

(1) Chen, C.; Kang, H.; Hsiao, S.; Yang, P.; Chiang, K.; Lin, H. Efficient and Uniform Planar-Type Perovskite Solar Cells by Simple Sequential Vacuum Deposition. *Adv. Mater.* **2014**, *26* (38), 6647–6652.

(2) Yoon, W.; Boercker, J. E.; Lumb, M. P.; Tischler, J. G.; Jenkins, P. P.; Walters, R. J. Vapor Deposition of Organic-Inorganic Hybrid Perovskite Thin-Films for Photovoltaic Applications. In *2014 IEEE 40th Photovoltaic Specialist Conference (PVSC)*; IEEE, 2014; pp 1577–1580.

(3) Zhang, W.; Saliba, M.; Moore, D. T.; Pathak, S. K.; Hörantner, M. T.; Stergiopoulos, T.; Stranks, S. D.; Eperon, G. E.; Alexander-Webber, J. A.; Abate, A.; et al. Ultrasmooth Organic–inorganic Perovskite Thin-Film Formation and Crystallization for Efficient Planar Heterojunction Solar Cells. *Nat. Commun.* **2015**, *6*, 6142.

(4) Wehrenfennig, C.; Liu, M.; Snaith, H. J.; Johnston, M. B.; Herz, L. M. Charge-Carrier Dynamics in Vapour-Deposited Films of the Organolead Halide Perovskite $CH_3NH_3PbI_{3-x}$–xCl_x. *Energy Environ. Sci.* **2014**, *7* (7), 2269–2275.

(5) Liu, M.; Johnston, M.; Snaith, H. Efficient Planar Heterojunction Perovskite Solar Cells by Vapour Deposition. *Nature* **2013**, *501* (7467), 395–398.

(6) Stranks, S. D.; Wood, S. M.; Wojciechowski, K.; Deschler, F.; Saliba, M.; Khandelwal, H.; Patel, J. B.; Elston, S. J.; Herz, L. M.; Johnston, M. B.; et al. Enhanced Amplified Spontaneous Emission in Perovskites Using a Flexible Cholesteric Liquid Crystal Reflector. *Nano Lett.* **2015**, *15* (8), 4935–4941.

(7) Pérez-Osorio, M. A.; Milot, R. L.; Filip, M. R.; Patel, J. B.; Herz, L. M.; Johnston, M. B.; Giustino, F. Vibrational Properties of the Organic–Inorganic Halide Perovskite $CH_3NH_3PbI_3$ from Theory and Experiment: Factor Group Analysis, First-Principles Calculations, and Low-Temperature Infrared Spectra. *J. Phys. Chem. C* **2015**, *119* (46), 25703–25718.

(8) Leguy, A. M. A.; Hu, Y.; Campoy-Quiles, M.; Alonso, M. I.; Weber, O. J.; Azarhoosh, P.; van Schilfgaarde, M.; Weller, M. T.; Bein, T.; Nelson, J.; et al. Reversible Hydration of $CH_3NH_3PbI_3$ in Films, Single Crystals, and Solar Cells. *Chem. Mater.* **2015**, *27* (9), 3397–3407.

(9) DeQuilettes, D. W.; Vorpahl, S. M.; Stranks, S. D.; Nagaoka, H.; Eperon, G. E.; Ziffer, M. E.; Snaith, H. J.; Ginger, D. S. Impact of Microstructure on Local Carrier Lifetime in Perovskite Solar Cells. *Science* **2015**, *348* (6235), 683–686.

(10) Lindsey, C. P.; Patterson, G. D. Detailed Comparison of the Williams–Watts and Cole–Davidson Functions. *J. Chem. Phys.* **1980**, *73* (7), 3348.